Available online at www.sciencedirect.com

ScienceDirect

Procedia Engineering 154 (2016) 1026 – 1033

Procedia Engineering

www.elsevier.com/locate/procedia

12th International Conference on Hydroinformatics, HIC 2016

Numerical simulation of 3D flow in right-angled confluences with bed elevation discordance in both converging channels

Dejana Đorđević[a]*, Ivan Stojnić[b,c]

[a]*Faculty of Civil Engineering, University of Belgrade, Bulevar kralja Aleksandra 73, 11000 Belgrade, Serbia*
[b]*(CERIS) - Instituto Superior Técnico - TU Lisbon, Avenida RoviscoPais 1, 1049-001, Portugal*
[c]*LCH – EPFL, Lausanne, Switzerland*

Abstract

The paper studies a combined effect of bed steps (BS) in both converging channels on the 3D flow in a confluence with $\alpha = 90°$. Nine combinations of bed elevation discordance ratio values in the two channels are analysed. It is shown that:1) a portion of the tributary flow is redirected upstream and that the vertical flow deflection in the lower half of water column is significantly reduced when the BS in the main river is higher than that in the tributary, 2) the shape of the recirculation zone (RZ) and the delay in its development are strongly governed by the presence of the BS in the tributary, whereas the BS in the main river only affects the size of the RZ and the dynamics of its distortion and 3) both river banks are endangered by erosion in confluences with BSs in both converging channels.

Peer-review under responsibility of the organizing committee of HIC 2016

Keywords: river confluence; bed elevation discordance; 3D numerical model

1. Introduction

Experimental observations of the channel bed morphology in movable bed models of confluences [1,14] revealed that channel bed configurations of different complexity might develop within the confluence and downstream of the confluence (in the post-confluence channel – PCC). It has been shown that the level of this complexity depends on a number of factors, or controls such as the confluence planform (symmetrical or asymmetrical), junction angle,

* Corresponding author. Tel.: +381-11-321-8560; fax: +381-11-337-0223.
E-mail address: dejana@grf.bg.ac.rs

Peer-review under responsibility of the organizing committee of HIC 2016
doi:10.1016/j.proeng.2016.07.592

momentum flux (or discharge) ratio of the converging flows, geological composition and sediment characteristics (i.e. the grain-size distribution and cohesiveness) of both the bed material and the sediment load. It is evident from these observations that, in addition to the bar which might form in the recirculation zone (RZ, Fig. 1b), there are two major morphological forms which can develop within the confluence hydrodynamic zone (CHZ). These are an avalanche of coarser sediments at the entrance of the upstream channel to the confluence and the scour hole in the PCC.

An avalanche face protrudes into a scour hole and creates the difference in bed elevations between the incoming and outgoing channels, i.e. the bed step (BS). Such a difference in bed elevations is usually referred to as bed elevation discordance. It may develop either at the entrance of one of or at the entrance of both converging channels to the confluence. Experiments have shown [1], and recent bathymetric surveys in a confluence of two large alluvial rivers with $\alpha \approx 80°$ confirmed [9], that avalanche faces (bed steps) developed at the entrance of both converging channels to the confluence when the junction angle was sufficiently large ($\alpha \geq 45°$).

The effect of the BS at the tributary entrance to the confluence on the confluence hydrodynamics was studied individually [2-7,10] and in combination with an upstream bend [8,11]. That of the bed elevation discordance in the main river was examined in [13]. The following step in the investigation of this important control to 3D flow and transport and mixing processes in river confluences is a study of the combined effect of the backward facing steps that are created in both converging channels at their entrance to the confluence. This analysis is performed in the present paper by using a 3D finite-volume based numerical model that was previously validated against experimental data of [3,17] and field data [9]. To facilitate comparison with previous studies, the confluence planform ($\alpha = 90°$) and cross-sectional geometries of the two channels ($B / h = 3.0$ in the case with no bed steps) are taken from Shumate's laboratory confluence (Fig. 1). Different extents of bed elevation discordance on the tributary and the main river sides are taken into account through consideration of nine combinations of bed-elevation-discordance-ratio values: $\Delta z_T / h_d = \{0.10, 0.25, 0.50\}$ and $\Delta z_{MR} / h_d = \{0.10, 0.25, 0.50\}$. Here Δz_T stands for the difference in bed elevations between the tributary and post-confluence channels (Fig. 2a), Δz_{MR} for the difference between stretches of the main river upstream and downstream of the upstream junction corner (Fig. 2b) and h_d for the flow depth in the main river at the confluence. The main channel (river) is divided into the upstream (shallower) and downstream (deeper) reaches at the upstream junction corner such that the vertical face of the bed step lies in the same plane as the tributary wall (Fig. 2c).

The combined effect of the two bed steps is analysed through comparison of the following key flow features in the CHZ: 1) the flow deflection on the horizontal and vertical planes at the tributary entrance to the confluence, 2) cross-sectional distributions of the three velocity components in the PCC and 3) variations of the size and orientation of the recirculation zone (RZ) throughout the flow depth.

2. Setup of numerical experiments

Since this paper is a continuation of previous studies [9,10,11,13], the confluence planform and channel geometries are taken again from Shumate's laboratory confluence (Fig. 1a). This is a right-angled confluence of two

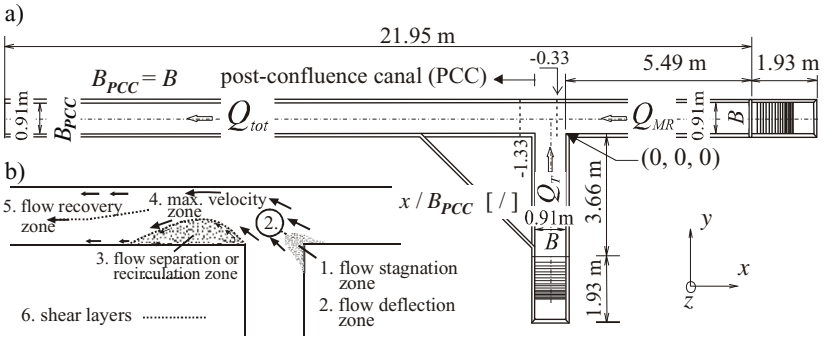

Figure 1. a) Plan view of Shumate's laboratory canal [17]; b) regions in the confluence hydrodynamics zone after Best [1] (from [11]).

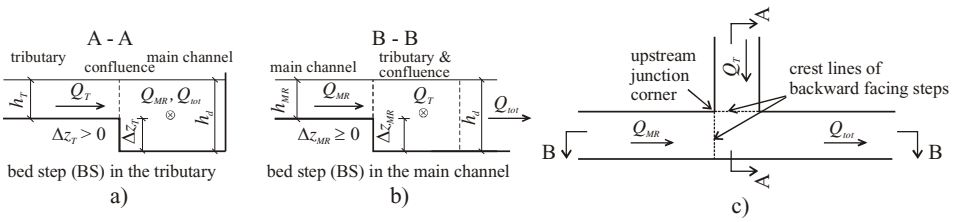

Figure 2. Definition sketch for the bed elevation discordance in: a) tributary; b) main channel; c) locations of backward facing steps in tributary and main channels.

straight, equal, width (B = 0.91 m) channels with horizontal non-deformable, flat beds. The selection of the junction angle α = 90° complies with the observed rule that the bed elevation discordance developed in both converging channels at their entrance to the confluence when $\alpha \geq 45°$. Nine hypothetical confluence layouts are prepared for this study by lifting the tributary (side-channel) bed for the amount Δz_T (Fig. 2a) above the bed of the PCC and by lifting the bed of the main river (channel) along upstream reach for the amount of Δz_{MR} (Fig. 2b). Each converging channel ends with the vertical backward facing step of the corresponding height. The vertical bed step face in the main river lies in the continuation of the tributary wall which ends at the upstream junction corner, whereas that in the tributary spans between two junction-corners (Fig. 2c). Bed step heights are chosen to cover a range of possible extents of bed elevation discordance between the converging and outgoing channels (see Table 1). The Δz / h_d value of 0.50 is the maximal observed value in river confluences.

The combined effect of the two BSs is studied for the discharge combination from Shumate's experiments which corresponds to the case with almost equal contributions of the converging flows, i.e. for $D_R = Q_{MR} / Q_{tot} = 0.583$ (see Fig. 1a). Such a choice is based on the results from previous studies which have shown that all six regions (recognised by Best [1]) might develop within the CHZ for this D_R-value. The total combined discharge and the flow depth at the downstream end of the main channel were the same in all Shumate's experiments (Q_{tot} = 0.17 m^3/s and h_{out} = 0.296 m). These values are used for numerical simulations in this study.

3. Numerical modelling

A 3D finite-volume based model SSIIM2 [15] which was successfully validated against Shumate's data [9,11,12] and applied in previous studies [10,11,13] is also used in this study. The model solves Reynolds-Averaged Navier-Stokes equations on unstructured space grids. SSIIM2 offers different types of two-equation turbulence models to close the problem. Since it was demonstrated in the model validation procedure that the best overall performance was achieved with the standard k-ε model, this model is used again in all numerical simulations.

An unstructured space grid on which the governing equations are solved may be composed of a number of smaller structured or unstructured space grids each of which covers a part of a complex flow domain. These smaller grids, which are usually called blocks, are glued together to give a single, multi-block grid of an arbitrary shape. A river confluence with its dendritic planform is a typical example of a complex flow domain which can be discretised with a multi-block grid. In the present case the multi-block grid has two blocks, each of which is an orthogonal structured grid. The block 1 covers the full length of the main channel, whereas block 2 covers the tributary channel. Block sizes on the horizontal plane are the same in all confluence layouts: 878×38 cells in the streamwise and lateral directions, respectively for the block 1 and 183×38 cells for the block 2. The block 1 has two distinct parts – the downstream part, which extends downstream of the upstream junction corner and the upstream part, which extends upstream of this

Table 1. Tags of considered confluence layouts and vertical grid sizes in the upstream part of block 1 and block 2, for considered bed elevation discordance ratio values.

Δz_{MR} / h_d [/]	Case No. Δz_T / h_d [/]			Vertical grid size
	0.10	0.25	0.50	
0.10	1	2	3	19
0.25	3	4	5	16
0.50	6	7	8	11

corner. The size of the downstream part, which covers the PCC is fixed: 658×38×21 cells in the streamwise, lateral and vertical directions. However, vertical sizes of the block 2 and the upstream part of block 1 vary with the change in the extent of the bed elevation discordance between each of the converging channels and the PCC (Table 1).

The confluence is an area with high velocity gradients. They additionally increase in the presence of BSs at the entrance of one or both converging channels to the confluence. This may pose some problems if convective terms are not properly discretised. Previous studies have shown that a better agreement with measurements is achieved when the second-order upwind scheme is applied for the discretisation of convective terms in the momentum equations [8,9,11]. Thus, the second-order upwind scheme is also used for numerical modelling of these terms in this paper. Since there is no other option available, the free-surface is treated with the rigid-lid approach. In such a case the continuity and momentum equations are coupled using the SIMPLE algorithm.

Considering the fact that Shumate's experiments were performed under the steady and subcritical flow conditions, all numerical simulations are based on these two assumptions. To ensure no influence of boundary conditions on the flow pattern in the CHZ, the computational domain covers full lengths of both channels. Boundary conditions include constant inflow discharges that are prescribed at upstream boundaries and a constant depth of 0.296 m, that is prescribed at the outflow boundary. The remaining dependent variables at the outflow boundary (i.e. three velocity components, (u, v, w), turbulence kinetic energy k and its dissipation rate ε) are calculated using the zero-gradient condition. This condition is also applied at the free-surface for all variables except the vertical velocity w and k. The w-velocity is determined from the zero-discharge condition, and k is set to half of its bottom value as explained in [15]. Boundary conditions along solid boundaries (bed and banks) are defined using the wall-law.

4. Results and discussion

The study of the combined effect of the two BSs begins with the analysis of numerical simulation results in the flow deflection zone, i.e.at the upstream end of the CHZ (Fig. 1b). The influence of BSs on the transfer of momentum of the tributary flow to the main channel is assessed through examination of distributions of flow deflection angles on the horizontal (δ = arc tg (v / u)) and vertical (φ = arc tg $[(u^2 + w^2)^{1/2} / w]$) planes (see definition sketches at the bottom of Fig. 3). The study continues with the observation of cross-sectional distributions of three velocity components in the confluence and the PCC and variations of the RZ size and its orientation throughout the flow depth.

Flow angles. Variations of flow angles δ and φ along the junction line are presented at four selected non-dimensional elevations (z / h_T) above the tributary bed (Fig. 3). In addition to the data from this study, each diagram is supplied with corresponding results for cases with no BS in the main channel ($\Delta z_{MR} = 0$, [10]). The following can be observed on δ-angle distributions. When the BS in the tributary is higher than that in the main river ($\Delta z_{MR} < \Delta z_T$), δ-angle distributions are almost independent of the presence of the BS in the main channel. However, in the bottom $0.25h_T$ the flow deflection near the upstream junction corner ($l < 0.20L_{u\text{-}d}$, see Fig. 3 for the definition of $L_{u\text{-}d}$) reduces in the presence of the BS in the main river (Fig. 3I, $\Delta z_T / h_d \geq 0.25$, $z / h_T = 0.008$). When $\Delta z_T = 0.25h_d$ δ-angle increases by approximately 25% ($\Delta z_{MR} = 0.10h_d$) at $z / h_T = 0.008$. For the $\Delta z_T = 0.50h_d$ the increase is almost 50% when $\Delta z_{MR} = 0.10h_d$, and the δ-angle value is doubled ($\approx$ 110 %) when $\Delta z_{MR} = 0.25h_d$. The reduced deflection of the flow from the shallower tributary is explained by essentially different pressure fields in the presence of the BS in the main river (Fig. 4). When there is no BS in the main river, a single, low pressure zone is developed near the downstream junction corner (Fig. 4, case 0). Bed elevation discordance in the main river gives rise to the development of an additional low pressure zone near the BS (Fig. 4, cases 3 and 6). Thus, the pressure in both low pressure zones is higher than that in the single zone. For example, when $\Delta z_T / h_d = 0.50$ the minimal pressure near the downstream junction corner is approximately 40% higher for $\Delta z_{MR} = 0.10h_d$ (case 3) and approximately 30% higher for $\Delta z_{MR} = 0.25h_d$ (case 6) than that in case 0. As it can be seen on Figure 4, large pressure gradients between high pressure zone (which extends on the main-river-side deep into the confluence and includes upstream junction corner) and the low pressure zone (near the downstream junction corner) force tributary streamlines to turn more rapidly when there is no BS in the main river (Fig. 4, case 0).

The BS in the main river which is higher than that in the tributary ($\Delta z_{MR} > \Delta z_T$) helps the tributary flow to keep its original direction at the upstream junction corner in layers bellow its crest ($z / h_T < \Delta z_{MR} / h_d$). Moreover, the additional low pressure zone, which develops below this step, redirects a portion of the tributary flow towards the BS (Fig. 4, case 3 to the right). The greater is the difference in the two step heights (i.e. $\Delta z_{MR} - \Delta z_T$) the greater is the

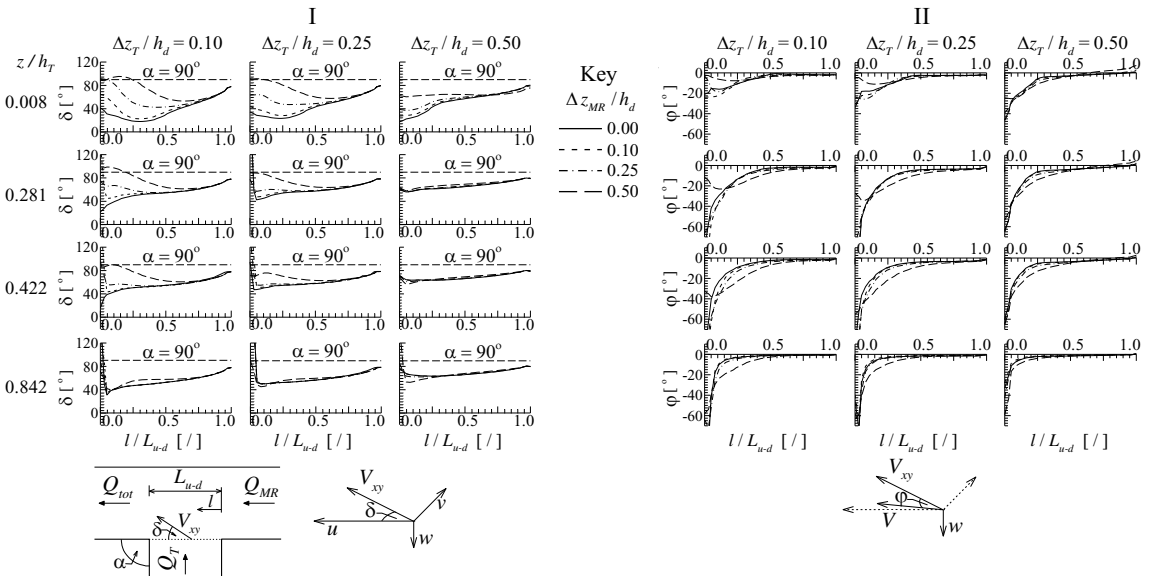

Figure 3. Effects of $\Delta z_{MR} / h_d$ and $\Delta z_T / h_d$ on: I) δ-angle and II) φ-angle distributions at tributary entrance to confluence (z / h_T is non-dimensional distance from the bottom of the tributary.

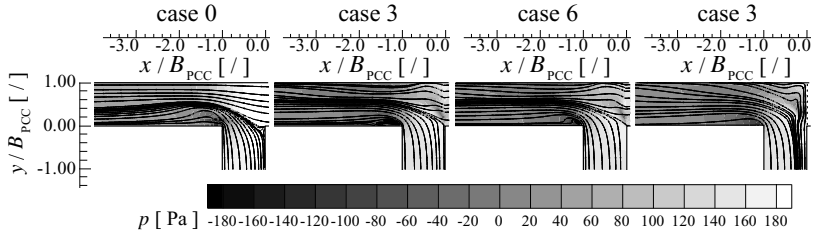

Figure 4. Effects of $\Delta z_{MR} / h_d$ and $\Delta z_T / h_d$ on the flow deflection on the horizontal plane; in case 0 there is no BS in main river; $z / h_d = 0.50$ in cases 0, 3 and 6 and $z / h_d = 0.10$ in case 3 to the right; streamlines are superimposed on pressure distributions.

portion of the redirected flow (δ > α). For example, when $\Delta z_T = 0.10 h_d$, flow is redirected from the upstream $0.05 L_{u\text{-}d}$ when $\Delta z_{MR} = 0.25 h_d$, and from ≈ $0.25 L_{u\text{-}d}$ when $\Delta z_{MR} = 0.50 h_d$ (Fig. 3I, $z / h_T = 0.008$). Consequently, the δ-angle reaches its maximum in this zone. The width of the zone of redirected flow reduces with distance from the tributary bed, and the locus of δ_{max} is moved upstream. The location of the corresponding minimum remains unaltered (for $\Delta z_T = 0.10 h_d$ and $\Delta z_{MR} = 0.50 h_d$, δ_{min} is reached at $0.65 L_{u\text{-}d}$, Fig. 3I). Above the crest level ($z / h_T > \Delta z_{MR} / h_d$) the whole tributary flow turns downstream and δ < α throughout the junction-line length.

Differences in δ-angle distributions for various channel bed configurations reduce from the mid-depth towards the free-surface when $\Delta z_T \leq 0.25 h_d$. The BS with $\Delta z_{MR} = 0.50 h_d$ causes a lesser deflection along the middle portion of the junction line when it is higher than BS in the tributary (Fig. 3I, $\Delta z_T / h_d = 0.25 h_d$).

Cases with the greatest extent of bed elevation discordance in the tributary ($\Delta z_T = 0.50 h_d$) are markedly different from those with $\Delta z_T \leq 0.25 h_d$. Significant differences between the four cases exist only in the bottom $0.25 h_T$ for $l < 0.65 L_{u\text{-}d}$. The δ-angle distributions are monotonously increasing lines with the minimum at the upstream junction corner ($\Delta z_{MR} \leq 0.25 h_d$). In the upper 70% of the water column δ-angle varies in a range [56°, 80°].

The combined effect of BSs in the tributary and the main river on the vertical flow deflection at the tributary entrance to the confluence is presented in Figure 3II. It is readily noticeable that the presence of the BS in the main river affects φ-angle distribution in the bottom $0.10 h_T$ when $\Delta z_{MR} > \Delta z_T$. The |φ|-angle value is significantly reduced near the upstream junction corner: 7-10 times when $\Delta z_T = 0.10 h_d$, 6 times when $\Delta z_T = 0.25 h_d$ and it is halved when

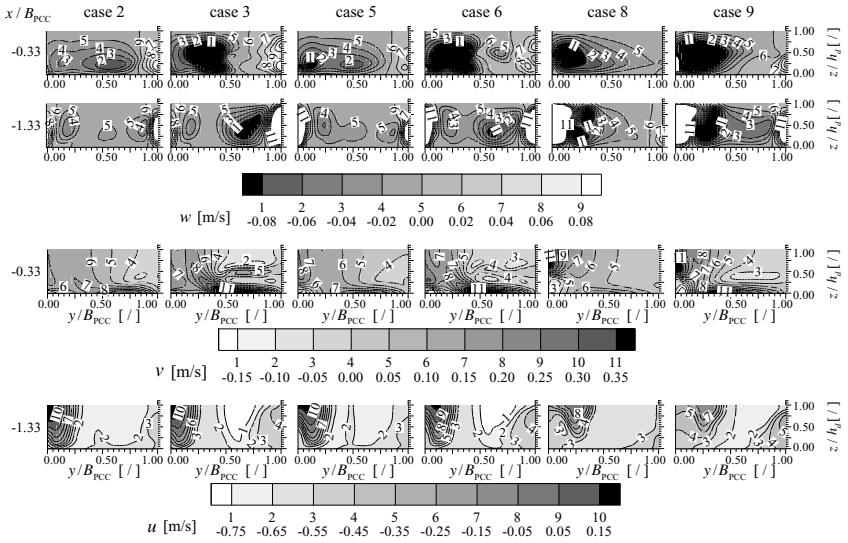

Figure 5. Effects of $\Delta z_{MR} / h_d$ and $\Delta z_T / h_d$ on the three velocity components in the confluence (x / B_{PCC} = -0.33) and downstream of the confluence (x / B_{PCC} = -1.33), see Fig. 1a.

$\Delta z_T = 0.50h_d$. Additionally, φ-lines, which are otherwise hyperbolic in shape turn to parabolae whose minima move towards the upstream junction corner with distance from the tributary bed (for the given Δz_{MR}-value) and with the decrease in Δz_{MR}. In the remaining part of the water column ($z > 0.10h_T$) only the highest BS in the main river ($\Delta z_{MR} = 0.50h_d$) affects φ-angle distributions when $\Delta z_T \leq 0.25h_d$. Even when the hyperbolic shape is established the step of this height causes 2-5 times greater vertical flow deflection then lower ones.

The flow is always directed towards the bottom except in the confluence with $\Delta z_T = \Delta z_{MR} = 0.50h_d$ where the flow locally turns upward (Fig. 3II, $z = 0.008h_T$, $l > 0.65L_{u\text{-}d}$). Generally, enhanced vertical flow deflection exits in the upstream half of the tributary cross-section. The deflection is significantly reduced or it is even negligible in the downstream half of the cross-section, which means that the bulk of the momentum of the tributary flow is transferred to the main channel through the horizontal plane.

Cross-sectional velocity distributions for the streamwise (u), lateral (v) and vertical (w) velocity components are shown in Figure 5. Since the distributions for $\Delta z_T \leq 0.25h_d$ are essentially the same, they are presented only for $\Delta z_T = 0.25h_d$ (cases 2, 5 and 8).

Vertical velocity distributions clearly indicate that the existence of the bed elevation discordance in the main river markedly affects flow pattern in the confluence and the PCC. Although the w-velocity reaches the same order of magnitude as V_{xy}-velocity (see Fig.3 for the explanation) in all confluence configurations, the 3D flow pattern is particularly enhanced when the extent of bed elevation discordance is at maximum (Fig. 5, cases 3, 6, and 9). Cores of high upward/downward velocities in these confluence configurations occupy half of the channel width, and extend throughout the flow depth. As already mentioned, the presence of the BS in the main river helps tributary streamlines, which would otherwise all turn downstream and align with the wall, to keep their original direction in the upstream portion of the junction line. Such a motion in the bottom layers is recognised on v-velocity distributions at x / B_{PCC} = - 0.33 (see Fig. 1a for the position of the cross-section) where the core of high velocities, that are oriented towards the opposite wall, occupies 0.10-0.22h_d, depending on the confluence layout. Upon reaching the wall, streamlines continue to move upward along the wall. This results in large upward w-velocity cores at the opposite wall (w-velocity distributions) in addition to those at the BS in the tributary and along the junction-side wall. Though the maximal w-velocity magnitude at the opposite wall is 3-4 times lower than that at the tributary bed step and the junction-side wall, the upward fluid movement along this wall persist far downstream of the confluence ($x > 3B_{PCC}$, not presented in Fig. 5).

Streamwise velocity distributions (last row of panels in Fig. 5) suggest that the recirculation flow is limited to the upper half of the water column – core of positive, upstream oriented u-velocities, if present, is located above 0.60h_d.

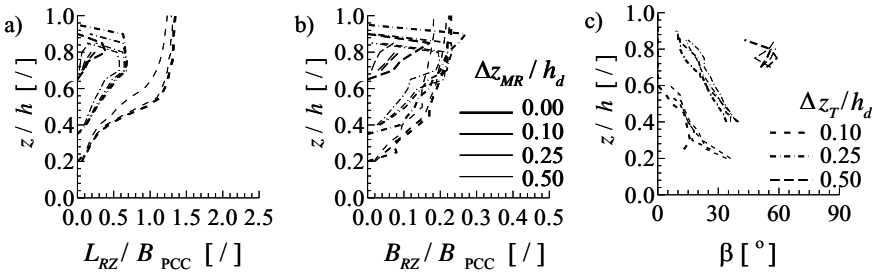

Figure 6. Effects of $\Delta z_{MR} / h_d$ and $\Delta z_T / h_d$ on recirculation zone length (L_{RZ}), width (B_{RZ}) and its inclination angle β.

The size of the core reduces and the core is lifted towards the free-surface as the height of either BS increases. Moreover, the core is moved away from the junction-side wall towards the channel axis with an increase in both BS heights, and one shear layer develops on each side of the core. The shear on the inner side is generally larger than that on the outer side ($(\Delta u / \Delta y)_{in}$ = 8.75 1/s and $(\Delta u / \Delta y)_{out}$ = 6.21 1/s for case 5). For the given $\Delta z_T / h_d$ both values reduce with the increase in Δz_{MR}. The core vanishes due to strong 3D flow in the PCC when $\Delta z_T = 0.50h_d$, regardless the Δz_{MR}-value (see panels for *w*-velocity in Fig. 5, cases 8 and 9).

As far as the core of high downstream velocities is concerned, there is a clear distinction between cases with $\Delta z_T \leq 0.25h_d$ and $\Delta z_T > 0.25h_d$. The following is observed when $\Delta z_T \leq 0.25h_d$. For the given Δz_T the $u_{\max}$-core distorts on the side of the opposite wall then Δz_{MR} increases. The distortion takes place due to enhancement of 3D flow, i.e. enlargement of upward *w*-velocity core at this wall (first two rows of panels in Fig. 5). Additionally, the $u_{\max}$ magnitude increases, and the core moves to the other half of the cross-section ($y / B_{PCC} \geq 0.50$). When $\Delta z_T = 0.50h_d$ (cases 8 and 9) there is no RZ. Thus, the $u_{\max}$ magnitude is lower than that in confluence with $\Delta z_T \leq 0.50h_d$. Again, the isovels distort with an increase in Δz_{MR}. Instead of being vertical, they are inclined towards the opposite wall.

Recirculation zone. The effect of two BSs on the size and orientation of the RZ is presented in Figure 6. It is readily noticeable that the shape of RZ and the delay in its development are strongly governed by the presence of the BS in the tributary. The BS in the main river only affects the size of RZ and the dynamics of its distortion.

When $\Delta z_T = 0.10h_d$ the RZ starts to develop $0.10h_d$ above the step crest and it exists up to the free-surface regardless the Δz_{MR}-value. The effect of the BS in the main river on the RZ is negligible as long as $\Delta z_{MR} \leq 0.25h_d$. However, when $\Delta z_{MR} = 0.50h_d$, the size is reduced. The greatest shortening (≈ 40%) happens around the mid-depth. Above this level RZ starts to elongate again. The maximal narrowing of 20% is attained at $0.60h$ and it is kept constant till the water-surface.

When $\Delta z_T \geq 0.25h_d$ the development is postponed by additional $0.05h$ (i.e. it starts $0.15h$ above the step crest) and the RZ is reduced in size. The RZ does not exist to the free-surface. It vanishes below the free-surface due to the enhanced 3D flow, as indicated on the cross-sectional velocity distributions in Figure 5. The increase in Δz_{MR} accelerates destruction of the RZ. In the confluence with $\Delta z_T = 0.25h_d$ the RZ vanishes at $0.95h$ when $\Delta z_{MR} = 0.0$ whereas for $\Delta z_{MR} = 0.50h_d$ the point of disappearance is lowered to $0.85h_d$. These levels are lowered to $0.90h$ ($\Delta z_{MR} = 0.00$) and $0.80h$ ($\Delta z_{MR} = 0.25h_d$) when $\Delta z_T = 0.50h_d$. As for the RZ size, the following can be concluded. The RZ maximal length (L_{RZ}) is successively halved with the increase in Δz_T. Its maximal width is not affected as long as $\Delta z_T \leq 0.25h_d$. However, in the confluence with $\Delta z_T = 0.50h_d$, the width (B_{RZ}) is reduced approximately 2.5-6.5 times when compared to $\Delta z_T = 0.25h_d$.

Detachment of the RZ from the junction-side wall results in the inclination of its longitudinal axis with respect to the channel axis. For $\Delta z_T \leq 0.25h_d$ the maximal inclination angle β is approximately the same ($\beta \in [35°, 38°]$) and it reduces with distance from the channel bed. When $\Delta z_T = 0.50h_d$ the β angle is much larger ($\beta \in [50°, 58°]$).

5. Conclusions

Nine channel bed configurations, characterised by various combinations of the bed elevation discordance ratio between the tributary and post confluence channels on one hand, and between the main channel upstream of the confluence and the post confluence channel on the other, have been investigated in 90° straight channels'

confluences using the 3D finite-volume based model with two-equation turbulence model closure. Numerical simulation results have shown the following.

1. When the BS in the tributary is higher than that in the main river, δ-angle distributions are independent of the presence of the BS in the main river.
2. When the BS in the main river is higher than that in the tributary, one part of the tributary flow is redirected towards the bed-step face in the layers below the step crest. The portion of the redirected flow increases with the increasing difference in BS heights. In addition, such a BS reduces vertical flow deflection in the lower half of the water column.
3. A strong 3D flow at the tributary entrance to the confluence is confined to the upstream part of the tributary cross-section. Thus, the bulk of momentum of the tributary flow is transferred in the horizontal plane through the downstream part of the cross-section.
4. The presence of the BS in the tributary causes a delay in the development of the RZ in the PCC (i.e. the zone starts to develop above the step crest) and affects its shape. However, the presence of the BS in the main river enhances 3D flow in the confluence and the PCC. This results in the detachment of the RZ from the junction-side wall. Such a RZ in no longer parallel with the wall. It is rather inclined at an angle to the main river axis.
5. The BS in the tributary enhances vertical velocities along the junction-side wall, while the BS in the main river enhances these velocities along the opposite wall. Thus, both river banks are endangered by erosion in confluences with bed elevation discordances in the two converging channels.

References

[1] J.L. Best, Sediment transport and bed morphology at river channel confluences, Sedimentology 35 (1988) 481-498.
[2] J.L. Best, A.G. Roy, Mixing-layer distortion at the confluence of channels of different depth, Nature 350 (1991) 411-413.
[3] P. Biron, J.L. Best, A.G. Roy, Effects of bed discordance on flow dynamics at open-channel confluences, J. Hydraul. Eng. ASCE, 122(12) (1996) 676-682.
[4] K.F. Bradbrook, P. Biron, S.N. Lane,K.S. Richards, A.G. Roy, Investigation of controls on secondary circulation in a simple confluence geometry using a three-dimensional numerical model, Hydrological Processes 12 (1998) 1371-1396.
[5] K.F. Bradbrook, S.N. Lane, K.S. Richards,P.M. Biron, A.G. Roy, Role of bed discordance at asymmetrical river confluences. J. Hydraul. Eng. ASCE, 127(5) (2001) 351-368.
[6] J.M. Gaudet & A.G. Roy, Effect of bed morphology on flow mixing length at river confluences. Nature 373 (1995) 138-139.
[7] B. De Serres, A.G. Roy, P.M. Biron, J.L. Best, Three-dimensional structure of flow at a confluence of river beds, Geomorphology 26 (1999) 313–335.
[8] D. Đorđević, P.M. Biron, Role of upstream planform curvature at asymmetrical confluences – laboratory exp-eriment revisited. Proc. 4th Int. Conference on Fluvial Hydraulics – River Flow 2008, Cesme, 3 (2008) 2277-2286.
[9] D. Đorđević, Numerical investigation of the river confluence hydrodynamics. Unpublished PhD Dissertation, University of Belgrade, Belgrade (2010).
[10] D. Đorđević,Numerical simulation of 3D flowat 90º straight channel confluence withbed elevation discordance. CD-ROM Proc. 10thInt. Conference on Hydroinformatics – HIC 2012, Hamburg (2012).
[11] D. Đorđević, Numerical study of 3D flow at right-angled confluences with and without upstream planform curvature. J. of Hydroinformatics 15.4 (2013) 1073-1088.
[12] D. Đorđević, Can a 3D-numerical models be a substitute to a physical model in estimating parameters of 1D-confluence models? CD-ROM Proc. 3rd IAHR-Europe Congress, Porto, Portugal (2014) 158-167.
[13] D. Đorđević, Numerical simulation of 3D flow at right-angled confluences with bed elevation discordance in the main river. CUNY Academic Works (2014) http://academicworks.cuny.edu/cc_conf_hic/67.
[14] M. P. Mosley, An experimental study of channel con-fluences. Journal of Geology 94 (1976) 535-562.
[15] N.R. Olsen, CFD Algorithms for Hydraulic Engineering. Trondheim: The Norwegian University of Science and Technology (2000).
[16] B.L. Rhoads, S.T. Kenworthy, Flow structure at an asymmetrical stream confluence. Geomorphology 11 (1995) 273–293.
[17] E.D. Shumate, Experimental description of flow at an open-channel junction. Unpublished Master thesis, Univ. of Iowa, Iowa (1998).